Metallophysics and Advanced Technologies
Металофіз. новітні технол.
Metallofiz. Noveishie Tekhnol.
2024, vol. 46, No. 2, pp. 97–109
https://doi.org/10.15407/mfint.46.02.0097
Reprints available directly from the publisher

PACS numbers: 61.50.Lt, 71.15.Ap, 71.15.Nc, 71.20.-b, 75.10.Lp, 75.50.Cc, 85.75.-d

The Solid Solutions of Heusler Alloys $(Pd_{1-x}Me_x)_2MnSn$ (Me = Co, Ni, $x = 0.0–1.0$): Energy, Charge, and Magnetic Characteristics

V. M. Uvarov, M. V. Uvarov, Y. V. Kudryavtsev, E. M. Rudenko, and I. M. Makeieva

G. V. Kurdyumov Institute for Metal Physics, NAS of Ukraine,
36 Academician Vernadsky Blvd.,
UA-03142 Kyiv, Ukraine

Information on the energy, charge, and spin characteristics of $Pd_{1-x}Me_xMnSn$ alloys (Me = Co, Ni, $x = 0.0–1.0$) is obtained using band calculations within the FLAPW (full-potential linearized augmented-plane-wave) model. As determined, an increase in the concentration of the cobalt or nickel atoms leads to an increase in the interatomic electron density inside the alloys. This results in both a concurrent reduction in the parameters of their crystal lattices and an increase in the binding energies of the atoms. The number of electrons Q within the atomic spheres of Pd, Mn, and Sn in cobalt-containing alloys exceeds the corresponding values for nickel-containing phases, and the dependences of Q exhibit a systematic tendency to increase with the growth of substitutional-atoms' concentrations. The observed polarization of valence electrons leads to the appearance of magnetic moments on the atoms of the alloys. The magnetic moments of metal atoms are ferromagnetically ordered, and their magnitude depends on the type and concentration of substitutional atoms.

Key words: band calculations, Heusler alloys, electronic structure, magnetic moments, polarized electronic states, spintronics.

За допомогою зонних розрахунків у моделю FLAPW (the full-potential linearized augmented-plane-wave) одержано інформацію про енергетичні, зарядові та спінові характеристики стопів $Pd_{1-x}Me_xMnSn$ (Me = Co, Ni,

Corresponding author: Viktor Mykolayovych Uvarov
E-mail: uvarov@imp.kiev.ua

Citation: V. M. Uvarov, M. V. Uvarov, Y. V. Kudryavtsev, E. M. Rudenko, and I. M. Makeieva, The Solid Solutions of Heusler Alloys $(Pd_{1-x}Me_x)_2MnSn$ (Me = Co, Ni, $x = 0.0–1.0$): Energy, Charge, and Magnetic Characteristics, *Metallofiz. Noveishie Tekhnol.*, **46**, No. 2: 97–109 (2024). DOI: 10.15407/mfint.46.02.0097

$x = 0{,}0–1{,}0$). Встановлено, що зі зростанням концентрації атомів Кобальту або Ніклю збільшується міжатомна густина електронів у стопах. Це забезпечує супровідне зменшення параметрів їхніх кристалічних ґратниць і підвищення енергій зв'язку атомів. Кількість електронів Q в атомових Pd-, Mn- і Sn-сферах у стопах з Кобальтом перевищує відповідні значення для фаз з Ніклем, а залежності Q виявляють систематичну тенденцію до збільшення зі зростанням концентрацій атомів заміщення. Виявлена поляризація валентних електронів приводить до появи магнетних моментів на атомах стопів. Магнетні моменти атомів металів феромагнетно упорядковані, а їхня величина залежить від типу та концентрації атомів заміщення.

Ключові слова: зонні розрахунки, Гойслерові стопи, електронна будова, магнетні моменти, поляризовані електронні стани, спінтроніка.

(Received 20 December, 2023; in final version, 10 January, 2024)

1. INTRODUCTION

Materials exhibiting unusual properties have always attracted significant attention from both theorists and experimentalists with the aim of harnessing these non-traditional properties for potential practical applications. One such group of materials currently under active investigation is the Heusler compounds (alloys, phases). Among them, there are the so-called the full-Heusler phases known as $L2_1$-type structures [1–7] have a common formula X_2YZ, where X and Y represent transition or noble metals, and Z is element of the IIIA (Al, Ga, In), IVA (Si, Ge, Sn) or VA (Sb) columns of the periodic table. This structure can be described by four interpenetrating f.c.c. sublattices: two of them occupied by the X atoms, and the other two by Y and the Z elements. The half-Heusler phases ($C1_b$-structures) have the same structure, except that one of the sites occupied by the X atom in the parent compound is empty, giving a general formula XYZ [5]. Both types of the mentioned phases have [9–12] a complex of magnetic, kinetic, optical, magnetooptical, superconducting, thermoelectric, and other important properties. In the system of compounds under discussion, it is possible to implement topological insulators and the so called half-metallic state of a solid with a completely uncompensated spin density of band electrons at the Fermi level—an important property necessary in technologies for creating materials for spintronics devices. The properties of Heusler phases significantly depend on their atomic composition, particularly the characteristics of the crystalline structure, atomic packing dimensions ($1D$, $2D$, $3D$), and so on.

The magnetic properties of Heusler alloys with variable atomic composition have always sparked enduring interest. The system of manganese-based Heusler alloys with the general formula X_2MnZ satisfies

this criterion [13–16]. Like most Heusler alloys, they are traditionally considered ideal systems with local atomic magnetic moments [13]. It is well known that the largest magnetic moment in the X_2MnZ phases is concentrated on manganese atoms and can reach values exceeding $4.0\mu_B$ [14–16]. In the structural ground state of these phases, Mn atoms are surrounded by eight first neighbours of type X and six second neighbours of type Z. Thus, the closest Mn–Mn pair is separated by two coordination atomic spheres. Due to the large distance between Mn atoms, it is commonly assumed [13] that their magnetic interaction occurs through free electrons in terms of indirect exchange, such as Ruderman–Kittel–Kasuya–Yosida (RKKY) exchange. The type of X atom plays a significant role in such exchange. It can be either nonmagnetic or magnetic. The transition from paramagnetic [17] or nearly magnetic [18] X = Pd to X = Ni (with an atomic magnetic moment $m_{Ni} = 0.604\mu_B$) and X = Co ($m_{Co} = 1.715\mu_B$) [17] is accompanied by a sequential decrease in the magnetic moment on manganese atoms in the Co_2MnSn alloy by almost 18% [16].

An effective way to influence the properties of Heusler phases is the synthesis of solid solutions based on them. Good model systems of this plan are a series of $Pt_{1-x}Me_xMnSb$ alloys (Me = Ni, Cu, Au, $x = 0.0–1.0$) ($C1_b$-structures) [19, 20]. In our earlier works [21–23], information about the energetic, charge, and spin characteristics of the mentioned alloys was obtained using the WIEN2k software package [24]. It has been established that with an increase in the concentration of Me-atoms, the electron density in the interatomic region of the compounds decreases, covalent bonds weaken, and the binding energies of atoms in the alloys decrease. At the same time, the main contribution to the formation of magnetic moments is made by the $3d$ electrons of manganese atoms and the polarization of electrons at the Fermi levels depends on the composition of the alloys.

An analogous system, but now with full-Heusler alloys, is represented by solid solutions with the atomic composition $(Pd_{1-x}Me_x)_2MnSn$ (Me = Co, Ni, $x = 0.0–1.00$). The boundary phases ($x = 0.0, 1.0$) are part of the family of already discussed alloys X_2MnZ (X = Co, Ni, Pd, Z = Sn). Solid solutions provide a unique opportunity to monitor the change in properties of these phases in the sequential process of their mutual transformation. Samples of the solutions were synthesized and certified as single-phase with an $L2_1$ structure in the work [25]. Here, it is established that the concentration dependences of crystal lattice parameters and Curie temperatures exhibit a linear decreasing and increasing trend, respectively. An increase in the concentrations of cobalt atoms is accompanied by a growth in the values of the ferromagnetic saturation moment by more than 19% in the Co_2MnSn alloy. However, in the transition from Pd_2MnSn to Ni_2MnSn, the author of the cited work observed a slight ($\cong 5\%$) decreasing trend in the depend-

ence of the ferromagnetic saturation moment.

Outside of the cited work, a number of comparative characteristics of the electronic structure of $(Pd_{1-x}Me_x)_2MnSn$ (Me = Co, Ni, $x = 0.0$–1.00) alloys have not been studied. There was no complete information about their energy characteristics, the spin and charge states of atoms, the nature of interatomic chemical bonds, the structure of valence bands and conduction bands.

This paper is devoted to finding answers to these problems.

2. THE METHODOLOGY OF THE CALCULATIONS

Electronic structure calculations of solid solutions $(Pd_{1-x}Mex)_2MnSn$ (Me = Co, Ni, $x = 0.0$–1.00) were performed by the LAPW method [26] with a gradient approximation of the electron density (GGA-generalized gradient approximation) in the form [27]. A spin-polarized version of this method was used to calculate the characteristics of the electronic structure [24].

To obtain concentration characteristics of the electronic structure of solutions for the initial phases Me_2MnSn (Me = Co, Ni, Pd), supercells with dimensions of 2×2×2 were constructed. In these supercells, atomic substitutions were performed, simulating the composition and structure of $(Pd_{1-x}Me_x)_2MnSn$ (Me = Co, Ni, $x = 0.0$–1.00) phases. In the final stage, calculations for all alloys were conducted using the spatial group $P1$ (No. 1).

The parameters a lattices of the $Pd_{1-x}Me_xMnSn$ alloys (Me = Co, Ni, $x = 0.0$–1.0) required for the calculations are borrowed from the experimental data, obtained in [25]. The radii (R_{mt}) of the MT (muffin-tin) atomic spheres were chosen from the consideration of minimizing the size of the inter-sphere region in the Co_2MnSb alloy, which has the smallest unit cell volume. For all alloys and all the atoms in them, these radii were 2.43 Bohr radiuses (1 Bohr radius = $5.2918 \cdot 10^{-11}$ m). When calculating the characteristics of the electronic structure of all alloys, 112 points in the irreducible parts of their Brillouin zones were used. APW + lo bases are used to approximate the wave functions of the $3d$ electrons of all atoms, and LAPW bases are used for the wave functions of the remaining valence electrons. The size of the basis set was determined by setting the product $R_{mt}K_{max} = 7.0$ (K_{max} is the maximum value of the inverse lattice vector).

The binding energies (cohesive energies) were calculated as the differences between the total energies of the atoms forming the unit cells of the alloys themselves, and the sum of the total energies of their constituent atoms, separated from each other by ‘infinity’. They were determined in accordance with the recommendations [28]. Test calculations of metal binding energies are presented in Fig. 1.

The obtained values of atomic binding energies in metals in this

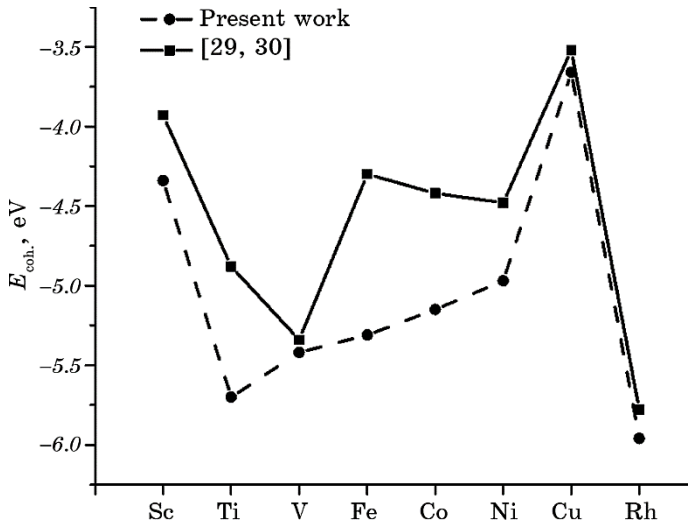

Fig. 1. Formation energy (cohesive energy $E_{coh.}$) of metals.

study exceed the corresponding values obtained from experiments [29, 30]. The largest differences in the specified values are characteristic for iron ($\Delta E_{coh.} = 1.01$ eV), titanium ($\Delta E_{coh.} = 0.82$ eV), cobalt ($\Delta E_{coh.} = 0.73$ eV), and nickel ($\Delta E_{coh.} = 0.49$ eV). Despite these differences, the trends of both curves are similar. This circumstance allows us to hope that the data and the conclusions drawn from them regarding cohesive energies of similar series of compounds, similar to the investigated solid solutions $(Pd_{1-x}Me_x)_2MnSn$ (Me = Co, Ni, $x = 0.0–1.00$), will be at least qualitatively correct.

3. RESULTS AND DISCUSSION

Concentration dependences of the spatial electron density in the interatomic region II [24], crystal cell parameters, and binding energies of alloys $(Pd_{1-x}Me_x)_2MnSn$ (Me = Co, Ni, $x = 0.0–1.0$) are presented in Fig. 2. It can be observed that with the increase in concentrations of substituting Me atoms, the negative charge of electrons in the interatomic region systematically increases. This increase leads to additional 'contraction' of ions of atoms towards each other and, as a result, to a reduction in crystal cell parameters a and an increase in binding energies of solid solutions $(Pd_{1-x}Me_x)_2MnSn$ (Me = Co, Ni, $x = 0.0–1.0$). The latter circumstance may indicate a potential increase in the thermodynamic stability of the discussed alloys with an increase in the concentration of substituting atoms in them. The mentioned stability is most pronounced for alloys with cobalt, as their binding energies ($E_{coh.}$) are

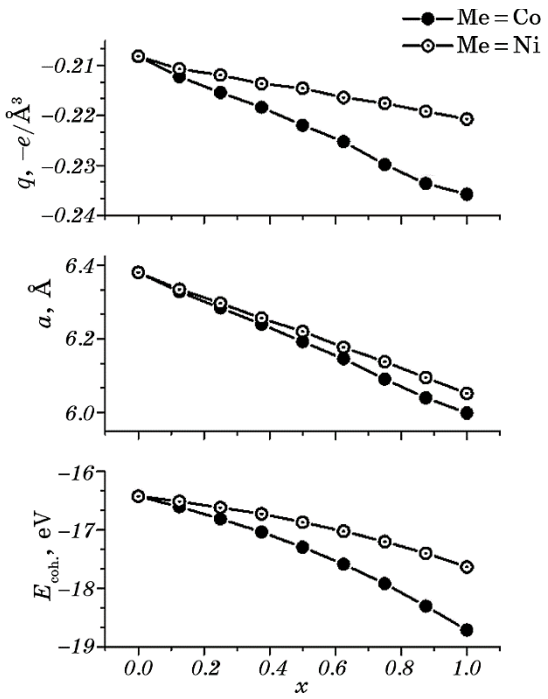

Fig. 2. Concentration dependences of electron densities q (e is electron charge) in the interatomic regions, parameters a [25] of conventional cells, and cohesive energies $E_{coh.}$ of $(Pd_{1-x}Me_x)_2MnSn$ ($x = 0.0–1.0$) alloys.

significantly higher compared to those for phases with nickel. It is also noteworthy that electron densities (q) and crystal cell parameters a depend on the type of Me-atoms. In phases with cobalt, the values of q throughout its concentration range exceed in magnitude the analogous values typical for nickel concentrations in alloys with its participation. This is also manifested in the smaller values of the lattice parameter a in the crystal structures of cobalt-containing alloys. The possible reason for the described dependences of the discussed characteristics on the type of substituting atoms is their 'ability' to participate in interactions with surrounding atoms. It seems that this ability of cobalt atoms is enhanced due to the more extended nature of their electron wave functions in response to the smaller charge of its nucleus compared to that of nickel.

The charge states of atoms Q (the number of electrons in MT spheres) in solid solutions with cobalt, for the same reason, exceed the corresponding values for phases with nickel (Fig. 3). The Q dependences show a systematically increasing trend across all ranges of concentrations of substituting Me-atoms. This correlates with the accompanying reduction in the lattice parameters a of the alloy crystal structures (Fig. 2), providing a 'pumping' of electron densities into atomic

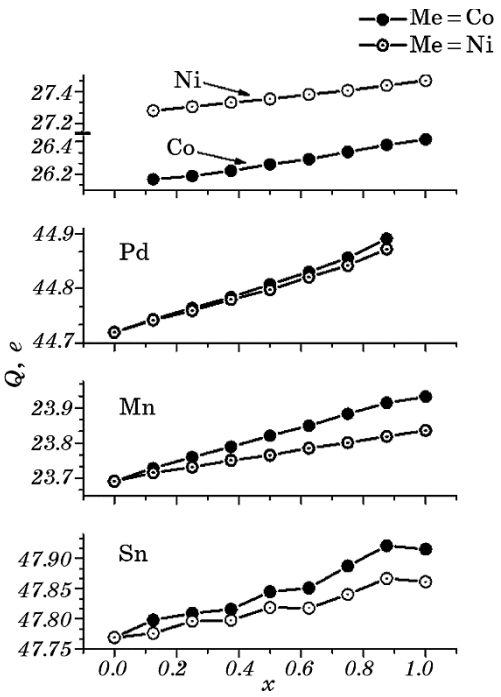

Fig. 3. Concentration dependences of atomic charges Q (e is electron charge) in $(Pd_{1-x}Me_x)_2MnSn$ ($x = 0.0–1.0$) alloys.

spheres. The 'sensitivity' of atoms to their recharging also depends on the type of substituting Me-atoms. In the transition across the concentration range $x = 0.0 \rightarrow x = 1.0$, the increase in atomic charges (ΔQ) was for cobalt-containing alloys $\Delta Q_{Co} = 0.9\%$, $\Delta Q_{Pd} = 0.4\%$, $\Delta Q_{Mn} = 1.0\%$, $\Delta Q_{Sn} = 0.3\%$, while for phases with nickel $\Delta Q_{Ni} = 0.7\%$, $\Delta Q_{Pd} = 0.3\%$, $\Delta Q_{Mn} = 0.6\%$, $\Delta Q_{Sn} = 0.2\%$.

Additional information about the nature of chemical bonds in the studied alloys can be obtained by considering the energy structure of their valence bands and zones of vacant states. The corresponding data in the form of curves representing the electron state densities are presented in Fig. 4. The total densities and total atomic densities of electronic states for the studied phases in both spin orientations are complex structures that vary depending on the atomic composition of the alloys. From the discussed figures, it can be seen that the influence of the alloys' atomic composition is manifested in the changing shape and energy localization of the densities of electronic states.

The electron densities from tin atoms in the localization region of valence states (0 to –5 eV) are insignificant, indicating a small ($\cong 4\%$) total charge of their valence electrons in the energy range of states that form interatomic bonds. This suggests that tin atoms in the crys-

tal lattices of the alloys are primarily held by ionic bonds.

The localization of the electronic states of metal atoms in this energy region and their hybridization indicate that the metal atoms in the alloys are bound together mainly by covalent interaction. Their further analysis is based on the basic principles of quantum chemistry [31]: in the absence of spatial symmetry constraints, the degree of interactions of the electrons entering into chemical bonds depends on the proximity of their energies and manifests itself in the energy splitting of the final states and the degree of their hybridization.

As seen in Fig. 4 for the Co_2MnSn and Ni_2MnSn alloys, the states of metal atoms occupy the same energy positions, hybridize well, and undergo energy splitting. These facts indicate a high degree of covalence in the Me–Mn chemical bonds, providing high values of the binding energy for the Me_2MnSn phases (Fig. 1). In the Pd_2Sn alloy, a somewhat different pattern of hybridization of electronic states of metal atoms is observed, which ultimately results in its reduced binding en-

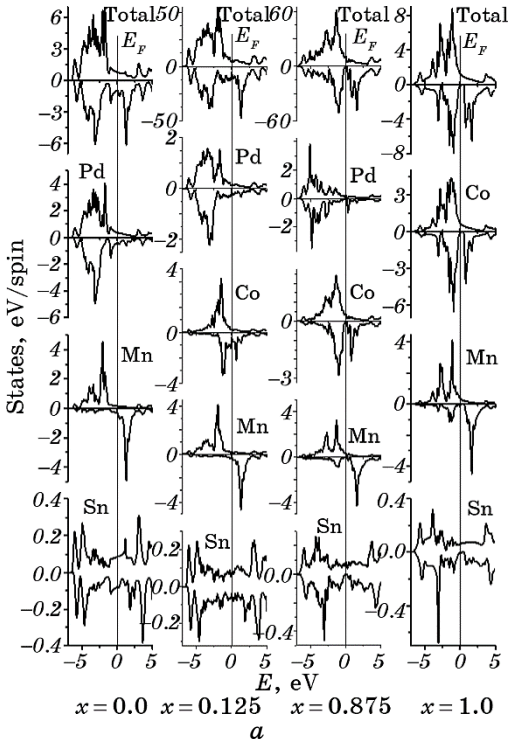

Fig. 4. Total electron densities (total) and total atomic electron densities of $Pd_{1-x}Me_xMnSn$ alloys: Me = Co (*a*), Me = Ni (*b*). Densities with positive and negative values correspond to the spin-up and spin-down orientations of the electrons respectively. E_F is the position of the Fermi level.

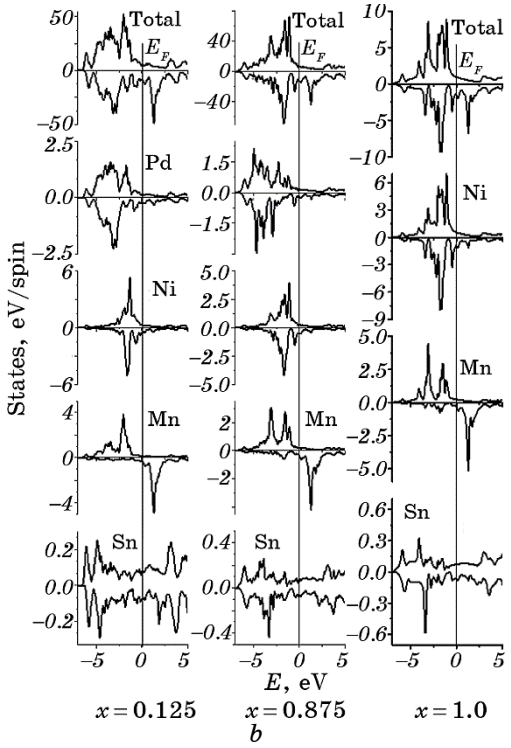

Continuation of Fig. 4.

ergy. It is also noteworthy (Fig. 4) that additional electronic densities from manganese atoms with negative spin values in the valence zone of Co_2MnSn exceed those for the alloy with Ni_2MnSn. This correlates with the increased binding energy of the cobalt-containing alloy compared to the nickel-containing alloy.

The concentration transition from Pd_2MnSn to Me_2MnSn (Me = Co, Ni) is accompanied by an increase in the hybridization of the Me atom states, while for the palladium atom states, the opposite trend is observed. The distributions of electron states of atoms in solid solutions with minimal concentrations of substituting Me atoms ($x = 0.125$) broadly replicate those of the Pd_2MnSn phase. In alloys with the maximum value of $x = 0.875$, the state distributions progressively form a pattern characteristic of Co_2MnSn and Ni_2MnSn. From the above, a qualitative assumption can be made that the increase in the binding energies of solid solutions $(Pd_{1-x}Me_x)_2MnSn$ with an increase in the concentrations of substituting Me atoms (Fig. 1) is due to the growing effects of hybridization of states of these atoms with the states of manganese atoms.

From Figure 4, it can also be inferred that the conduction band

states of the alloys are mainly formed by electrons of manganese atoms with a spin orientation downwards. Attention is drawn to the discrepancy in the shapes and values of electron densities associated with different spin directions, indicating the polarization of electronic states. This effect is most pronounced in manganese.

Polarization effects lead to the appearance of magnetic moments (M) on atoms and, overall, in the crystal cells of the investigated alloys. Concentration dependences of magnetic moments are shown in Fig. 5. As evident, their values are also influenced by the type of substituting Me-atoms. In alloys with cobalt, the magnitudes of M undergo more significant concentration changes compared to phases with nickel. When transitioning to maximum Me concentrations, magnetic moments on cobalt atoms decrease by $\cong 25\%$, while on nickel atoms, the decrease is only 6% (upper panel in Fig. 5). As for the magnetic moments of formula units, in the case of alloys with cobalt, they increase from $M_{\text{f.u.}} = 4.16\mu_B$ (Pd_2MnSn) to $M_{\text{f.u.}} = 5.03\mu_B$ (Co_2MnSn), reaching a maximum of $M_{\text{f.u.}} = 5.35\mu_B$ at a cobalt concentration of $x = 0.75$. However, the transition from Pd_2MnSn to Ni_2MnSn reduces the magnetic moment values to $M_{\text{f.u.}} = 4.07\mu_B$. It is worth noting that these values are in good agreement with experimentally obtained results:

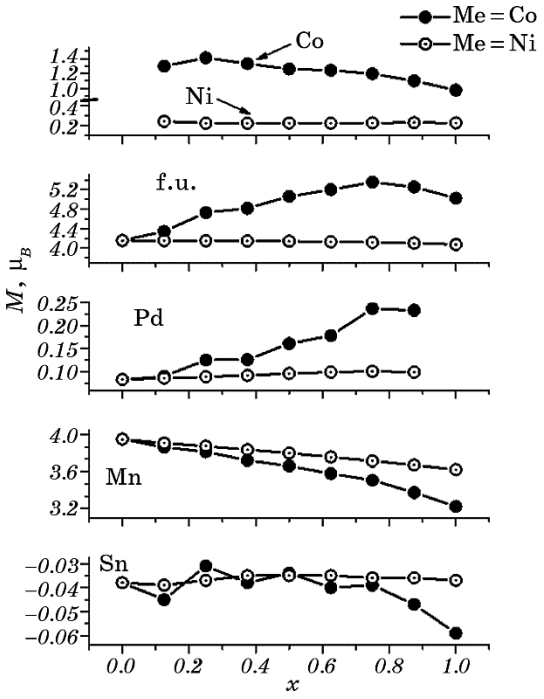

Fig. 5. Concentration dependences of magnetic moments M (μ_B is Bohr magneton) of atoms and formula units (f.u.) of $(Pd_{1-x}Me_x)_2MnSn$ ($x = 0.0–1.0$) alloys.

$M_{f.u.} = 4.23\mu_B$ [6], $M_{f.u.} = 5.08\mu_B$ [32], and $M_{f.u.} = 4.05\mu_B$ [6] for alloys with palladium, cobalt or nickel, respectively.

The changes in the magnetic moments on palladium atoms in alloys with nickel, as the concentration of substituting Me-atoms reaches its maximum, are small: $M_{Pd} = 0.08\mu_B$ (Pd_2MnSn) and $M_{Pd} = 0.10\mu_B$ (concentration $x = 0.875$). For phases with cobalt, the corresponding values increase to $M_{Pd} = 0.23\mu_B$.

The greatest contributions to the magnetism of the investigated alloys are made by manganese atoms. In both cobalt and nickel alloys, the concentration dependences of M_{Mn}, magnetic moments, exhibit a decreasing trend. For cobalt alloys, the magnetic moments on manganese atoms vary from $M_{Mn} = 3.95\mu_B$ (Pd_2MnSn) to $M_{Mn} = 3.22\mu_B$ (Co_2MnSn), while for nickel phases, the magnetic moment on manganese reaches the value of $M_{Mn} = 3.62\mu_B$ (Ni_2MnSn). In band calculations [13], similar values were obtained for these quantities: $M_{Mn} = 3.78\mu_B$ (Pd_2MnSn), $M_{Mn} = 3.13\mu_B$ (Co_2MnSn), and $M_{Mn} = 3.39\mu_B$ (Ni_2MnSn).

The magnetic moments on tin atoms (M_{Sn}) are antiferromagnetically ordered and have small values. In nickel-containing alloys, they practically do not depend on the concentrations of substituting nickel atoms, fluctuating slightly near $M_{Sn} = -0.036\mu_B$. For phases with cobalt, these magnetic moments undergo changes ranging from $M_{Sn} = -0.031\mu_B$ (Pd_2MnSn) to $M_{Sn} = -0.059\mu_B$ (Co_2MnSn).

4. CONCLUSIONS

1. With an increase in the concentration of cobalt or nickel in alloys $(Pd_{1-x}Me_x)_2MnSn$ (Me = Co, Ni, $x = 0.0–1.0$), the electron density in the space between atoms increases, leading to enhanced interatomic interactions and, consequently, a reduction in the lattice parameters of the alloys and an increase in their binding energies. These energies for cobalt-containing alloys exceed those for phases with nickel.
2. The number of electrons Q in the MT spheres of Pd-, Mn-, and Sn-atoms in solid solutions $(Pd_{1-x}Me_x)_2MnSn$ (Me = Co, Ni, $x = 0.0–1.0$) with cobalt exceeds the corresponding values for phases with nickel. The Q dependences exhibit a systematically increasing trend with the growth of substituting Me-atoms' concentrations. This correlates with the simultaneous reduction of the lattice parameters of the alloys, providing an 'injection' of electron densities into atomic spheres.
3. The densities of the electronic states of $(Pd_{1-x}Me_x)_2MnSn$ (Me = Co, Ni, $x = 0.0–1.0$) alloys are complex structures that vary in shape, energy position and localization. The zones of valence electrons (0––5 eV) of alloys are dominated by hybridized states of metals, while the vacant states are formed mainly by Mn electrons with spins oriented downwards.
4. The polarization of valence electrons leads to the emergence of mag-

netic moments on atoms in alloys $(Pd_{1-x}Me_x)_2MnSn$ (Me = Co, Ni, $x = 0.0–1.0$). The magnetic moments of metal atoms are ferromagnetically ordered and their magnitudes depend on the type and concentrations of substituting Me-atoms.

REFERENCES

1. F. Heusler, *Verh. Dtsch. Phys. Ges.*, **5**: 219 (1903).
2. D. F. Oxley, R. S. Tebble, and F. C. Williams, *J. Appl. Phys.*, **34**: 1362 (1963).
3. P. J. Webster, *Contemp. Phys.*, **10**: 559 (1969).
4. F. A. Hames and J. Crangle, *J. Appl. Phys.*, **42**: 1336 (1971).
5. G. E. Bacon and J. S. Plant, *J. Phys. F: Metal Phys.*, **1**: 524 (1971).
6. C. C. M. Campbell, *J. Phys. F: Metal Phys.*, **5**: 1931 (1975).
7. P. J. Webster, K. R. A. Ziebeck, S. L. Town, and M. S. Peak, *Phil. Mag. B*, **49**: 295(1984).
8. K. R. A. Ziebeck and P. J. Webster, *J. Phys. F: Metal Phys.*, **5**: 1756 (1984).
9. T. Graf, C. Felser, and S. S. P. Parkin, *Progress in Solid State Chem.*, No. 39: 1 (2011).
10. I. Galanakis, P. H. Dederichs, and N. Papanikolaou, *arXiv:cond-mat/0203534v3* (2002).
11. C. Felser, G. H. Fecher, and B. Balke, *Angew. Chem. Int. Ed.*, No. 46: 668 (2007).
12. I. Galanakis and P. H. Dederichs, *Lect. Notes Phys.*, **676**: 1 (2005).
13. J. Kubler, A. R. Williams, and C. B. Sommers, *Phys. Rev. B*, **28**, No. 4: 1745 (1983).
14. S. Plogmann, T. Schlatholter, J. Braun, M. Neumann, Yu. M. Yarmoshenko, M. V. Yablonskikh, E. I. Shreder, E. Z. Kurmaev, A. Wrona, and A. Ślebarski, *Phys. Rev. B*, **60**, No. 9: 6428 (1999).
15. Y. Kurtulus, M. Gilleben, and R. Dronskowski, *J. Comput. Chem.*, **27**: 90 (2006).
16. F. Aguilera-Granja, R. H. Aguilera-del-Toro, and J. L. Moran-Lopez, *Mater. Research Express*, **6**, No. 10: 1 (2019).
17. *Fizika Tverdogo Tela: Ehntsiklopedicheskiy Slovar'* [Solid State Physics: Encyclopaedic Dictionary] (Kiev: Naukova Dumka: 1998) (in Russian).
18. A. A. Povzner, A. G. Volkov, and A. N. Filanovich, *Fizika Tverdogo Tela*, **52**, No. 10: 1879 (2010) (in Russian).
19. P. P. J. van Engelen, D. B. de Mooij, J. H. Wijngaard, and K. H. J. Buschow, *J. Magn. Magn. Mater.*, **130**: 247 (1994).
20. H. Masumoto and K. Watanabe, *Trans. JIM*, **17**: 588 (1976).
21. V. N. Uvarov, N. V. Uvarov, V. V. Zagorodnii, and A. S. Kruk, *Ukr. J. Phys.*, **67**, No. 5: 327 (2022).
22. V. M. Uvarov and M. V. Uvarov, *Metallofiz. Noveishie Tekhnol.*, **44**, No. 8: 975 (2022).
23. V. M. Uvarov, M. V. Uvarov, and M. V. Nemoskalenko, *Metallofiz. Noveishie Tekhnol.*, **45**, No. 4: 443 (2023).
24. P. Blaha, K. Schwarz, G. K. Madsen, D. Kvasnicka, J. Luitz, R. Laskowsk, F. Tran, and L. D. Marks, *WIEN2k, An Augmented Plane Wave +Local Orbitals Program for Calculating Crystal Properties* (Wien: Techn. Universität: 2001).

25. E. Uhl, *Solid State Communications*, **53**, No. 4: 395 (1985).
26. D. Singh, *Plane Waves, Psedopotentials and LAPW Method* (Kluwer Academic: 1994).
27. J. P. Perdew, S. Burke, and M. Ernzerhof, *Phys. Rev. Lett.*, **77**: 3865 (1996).
28. http://www.wien2k.at/reg_user/faq
29. Ch. Kittel, *Einfuhrung in die Festkorperphysik* (Munchen: Oldenbourg Verlag: 1983), p. 92.
30. L. Schimka, J. Harl, and G. Kresse, *J. Chem. Phys.*, **134**: 024116 (2011).
31. J. N. Murrell, S. F. A. Kettle, and J. M. Tedder, *Teoriya Valentnosti* [Valence Theory] (Moskva: Mir: 1968) (Russian translation).
32. P. J. Webster, *J. Phys. Chem. Solids*, **32**: 1221 (1971).